

## Supplementary Information

### Nitrogen and Sulphur Co-doped Crumbled Graphene for Oxygen Reduction Reaction with Improved Activity and Stability in Acidic Medium†

Siddheswar N. Bhangé<sup>a</sup>, Sreekuttan M. Unni<sup>a,b</sup> and Sreekumar Kurungot<sup>\*a,c</sup>

<sup>a</sup>. Physical and Materials Chemistry Division, CSIR-National Chemical Laboratory, Pune, Maharashtra, India-411008. Email. k.sreekumar@ncl.res.in.

<sup>b</sup>. Chemical Resources Laboratory, Tokyo Institute of Technology, R1-17, 4259 Nagatsuta, Midori-ku, Japan.

<sup>c</sup>. Academy of Scientific and Innovative Research (AcSIR), CSIR-NCL Campus, Pune, Maharashtra, India-411008.

#### Materials Characterization:

Morphology of the synthesized materials was analyzed using a transmission electron microscope (TEM) Tecnai-T 20 model at an acceleration voltage of 200 kV. TEM sample was prepared by drop coating of well dispersed catalyst sample in isopropyl alcohol solution onto a carbon-coated Cu grid followed by drying. Rigaku Smartlab diffractometer was used for X-ray diffraction (XRD) of the samples at a scan rate of  $2^\circ \text{ min}^{-1}$ , for Cu K $\alpha$  radiation ( $\lambda = 1.5406 \text{ \AA}$ ). Thermogravimetric analysis (TGA) was carried out in air at  $900^\circ \text{C}$  with a heating rate of  $10^\circ \text{C min}^{-1}$ . VG Microtech Multilab ESCA 3000 spectrometer (Mg K $\alpha$  X-ray source ( $h\nu = 1.2536 \text{ keV}$ )) was used for X-ray photoelectron spectroscopy (XPS) of the catalysts. Raman analysis

was performed using an HR 800 Raman spectrometer (Jobin Yvon, Horiba, France) at 632 nm red laser (NRS 1500 W).

### **Electrochemical studies:**

The electrochemical analysis was carried out in a BioLogicSP-300 Potentio-Galvanostat using a three-electrode system with a glassy carbon electrode (GCE) as the working electrode, graphite rod and Hg/HgSO<sub>4</sub> as the counter and reference electrode, respectively. For the preparation of the catalyst ink, 10 mg of the material was dispersed in 1 ml solution of 3:1 ratio of IPA : water and 40 µl of 5 wt. % Nafion solution and sonicated for 1 h using a bath sonicator. For preparing the working electrode, 10 µl of the catalyst ink was drop coated on the glassy carbon electrode and dried under an IR lamp to get uniform coating on the electrode surface. The total catalyst loading on the glassy carbon electrode is 0.5 mg cm<sup>-2</sup>. 40 wt.% Pt/C with a catalyst loading of 0.2 mg cm<sup>-2</sup> was used for the comparison purpose in the half cell studies. The linear sweep voltammetry (LSV) was carried out in oxygen saturated 0.5 M H<sub>2</sub>SO<sub>4</sub> at a scan rate of 10 mV s<sup>-1</sup> with an electrode rotation rate of 1600 rpm.

### **Rotating Ring Disc Electrode (RRDE) Analysis:**

RRDE study was performed in an oxygen saturated 0.5 M H<sub>2</sub>SO<sub>4</sub> at a scan rate of 10 mV s<sup>-1</sup> with an electrode rotation speed of 1600 rpm. The ring potential was held at 1.5 V with respect to RHE. The collection efficiency of the ring was measured to be 0.37 using K<sub>3</sub>Fe(CN)<sub>6</sub> solution. The following equations were used to calculate the hydrogen peroxide percentage (mol %) and number of electrons:

$$H_2O_2 \% = \frac{200 \times I_R}{I_D + \frac{I_R}{N}} \text{----- (1)}$$

$$n = \frac{(4 \times I_D)}{(I_D + \frac{I_R}{N})} \text{-----} (2)$$

where,  $I_D$  is the disc current,  $I_R$  is the ring current and  $N$  is the collection efficiency.

### **Single cell analysis:**

Nafion 212 membrane was used as the proton conducting membrane and the membrane pre-treatment was performed as reported earlier.<sup>S1</sup> Conventional brush coating method was adopted for the preparation of the electrodes. For the cathode, a catalyst slurry was prepared by mixing PF-1000 and Nafion 20 wt.% (DuPont, USA) in isopropyl alcohol. Carbon to Nafion ratio in the catalyst was fixed as 0.5. The catalyst slurry was applied onto the gas diffusion layer (SGL, Germany) until a total loading of the catalyst reached as  $3 \text{ mg cm}^{-2}$ . For the anode, Pt/C (40 wt.%) was used as the catalyst with a Pt loading of  $0.5 \text{ mg cm}^{-2}$ . For comparison purpose, an MEA with the cathode comprising the standard Pt/C (40 wt.%) catalyst was also prepared by maintaining a Pt loading of  $0.5 \text{ mg cm}^{-2}$ .

Membrane electrode assembly (MEA) with  $4 \text{ cm}^2$  active electrode area was prepared by keeping the membrane in between the electrode and hot pressed at a temperature of  $130 \text{ }^\circ\text{C}$  with a pressure of 0.25 ton for 1 min. The prepared MEA was assembled using a standard fixture (Fuel Cell Technologies, USA) and the testing was performed by using a fuel cell test station (Fuel Cell Technologies Inc., Albuquerque, NM). Hydrogen and oxygen gas were used as the fuel and oxidant, respectively. These gases were delivered at a flow rate of 0.3 slpm for  $\text{H}_2$  and 0.5 slpm for  $\text{O}_2$  in the anode and cathode compartments, respectively, of the single cell. The single cell was analysed at a cell temperature of  $65 \text{ }^\circ\text{C}$  and 100 % humidity without applying any back-pressure.

Table S1: Surface elemental composition of the PF electrocatalysts calculated from XPS.

	C (atom %)	O (atom %)	N (atom %)	S (atom %)	Fe (atom %)
PF-800	80.86	12.02	4.39	2.47	0.24
PF-900	82.45	11.19	4.20	1.91	0.23
PF-1000	85.31	10.08	2.63	1.77	0.18

Table S2: Atom percentage of the different nitrogen coordinations in the PF electrocatalysts as calculated from XPS.

	Nitride (atom %)	Pyridinic (atom %)	Pyrrolic (atom %)	Graphitic (atom %)	Oxide (atom %)
PF-800	12.00	27.74	23.35	26.48	10.43
PF-900	14.86	19.24	24.50	24.59	16.40
PF-1000	9.17	12.50	18.38	28.00	32.00

Table S3: Electrochemical performance of the PF electrocatalysts in 0.5 M H<sub>2</sub>SO<sub>4</sub> in comparison with Pt/C (40 wt.%).

	Onset potential (V vs RHE)	Half-wave potential (V vs RHE)	Tafel slope (mV/decade)	Mass activity @ 0.85 V (A/g)
PF-1000	0.890	0.75	93	0.78
PF-900	0.890	0.75	94	0.70
PF-800	0.870	0.72	116	0.60
PFC-900	0.794	0.50	131	0.00
PAPS-900	0.843	0.56	126	0.00
Pt C (40 wt.%)	0.989	0.83	88	11.50

Table S4. ORR activity performance of PF-1000 in comparison with the reported non-precious catalysts in acidic medium.

	<b>Electrolyte</b>	<b>Onset Potential</b>	<b>Half wave potential</b>	<b>Catalyst loading</b>	<b>Catalysts</b>	<b>Reference</b>
1	<b>0.5 M H<sub>2</sub>SO<sub>4</sub></b>	<b>0.89 V vs. RHE</b>	<b>0.75 V vs. RHE</b>	<b>0.5 mg cm<sup>-2</sup></b>	<b>PF-1000</b>	<b>Present work</b>
2	0.1 M HClO <sub>4</sub>	0.77 V vs. RHE	-	-	FeS <sub>2</sub>	S 2
3	0.1 M HClO <sub>4</sub>	0.65 V vs. Ag/AgCl	-	~0.07 mg cm <sup>-2</sup>	Fe-NSG	S 3
4	0.5 M H <sub>2</sub> SO <sub>4</sub>	0.790 V vs. RHE	0.680 V vs. RHE	~0.40 mg cm <sup>-2</sup>	(FeSO <sub>4</sub> -PEI) LH	S 4
5	0.1 M HClO <sub>4</sub>	~0.35V vs Ag/AgCl	-	~0.153 mg cm <sup>-2</sup>	GIL-carbon	S 5
6	0.5 M H <sub>2</sub> SO <sub>4</sub>	0.80 V vs. RHE	-	~0.285 mg cm <sup>-2</sup>	Co <sub>1-x</sub> S/RGO	S 6
7	0.1M HClO <sub>4</sub>	0.90 V vs. RHE	0.75 V vs. RHE	0.6 mg cm <sup>-2</sup>	Fe-N-C	S 7
8	0.5 M H <sub>2</sub> SO <sub>4</sub>	0.92 V vs. RHE	0.67 V vs. RHE	0.6 mg cm <sup>-2</sup>	PANI-Fe-C HT2	S 8
9	5.0 M H <sub>3</sub> PO <sub>4</sub>	0.92 V vs. RHE	0.77 V vs. RHE	0. mg cm <sup>-2</sup>	PANI-Fe-Kj	S 9
10	0.1 M HClO <sub>4</sub>	0.84 V vs. RHE	-	0.0395 mg cm <sup>-2</sup>	Fe-P	S 10

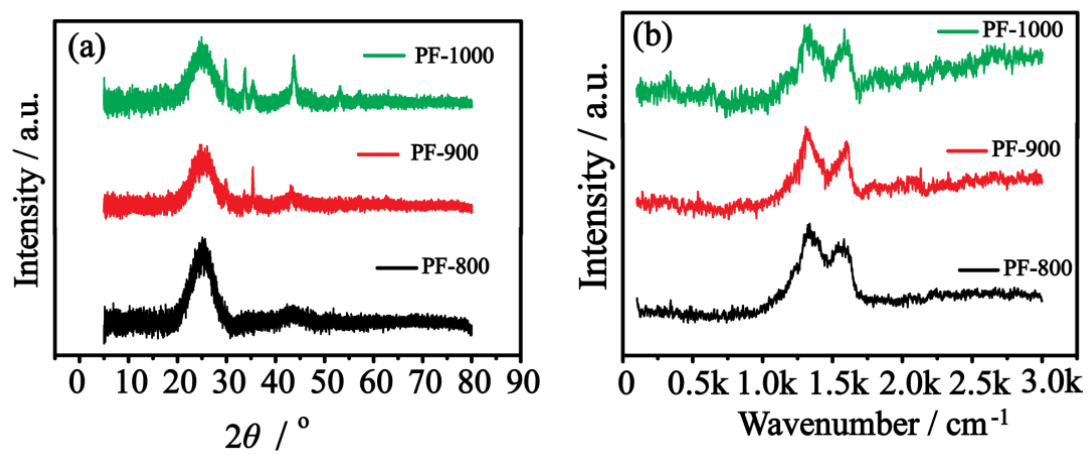


Figure S1. (a) X-ray diffraction (XRD) profiles and (b) Raman spectra of the PF electrocatalysts.

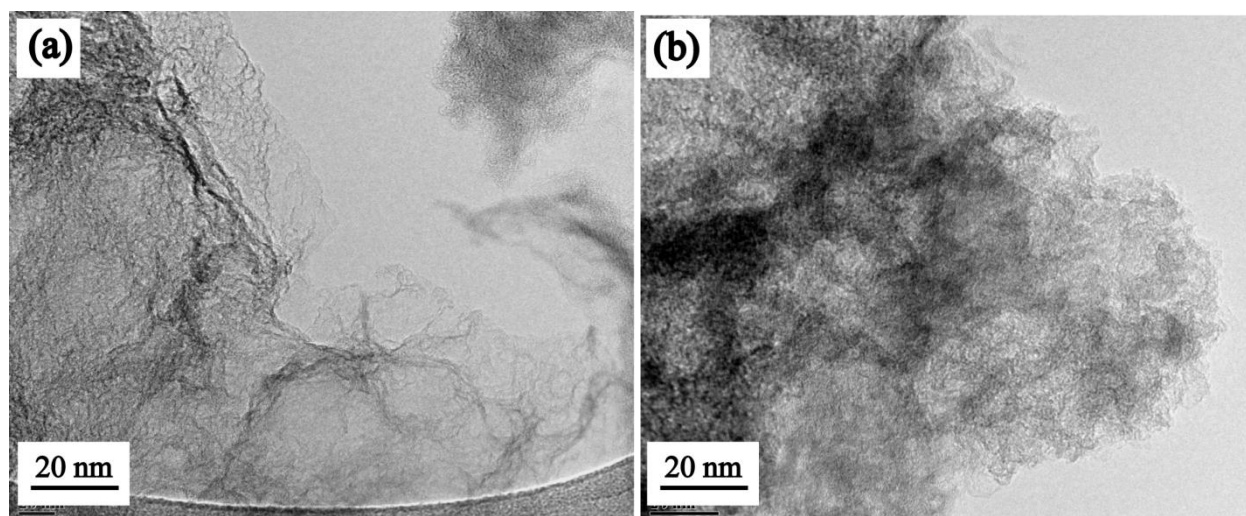


Figure S2. Transmission Electron Microscopic (TEM) images of the PF-1000 electrocatalysts.

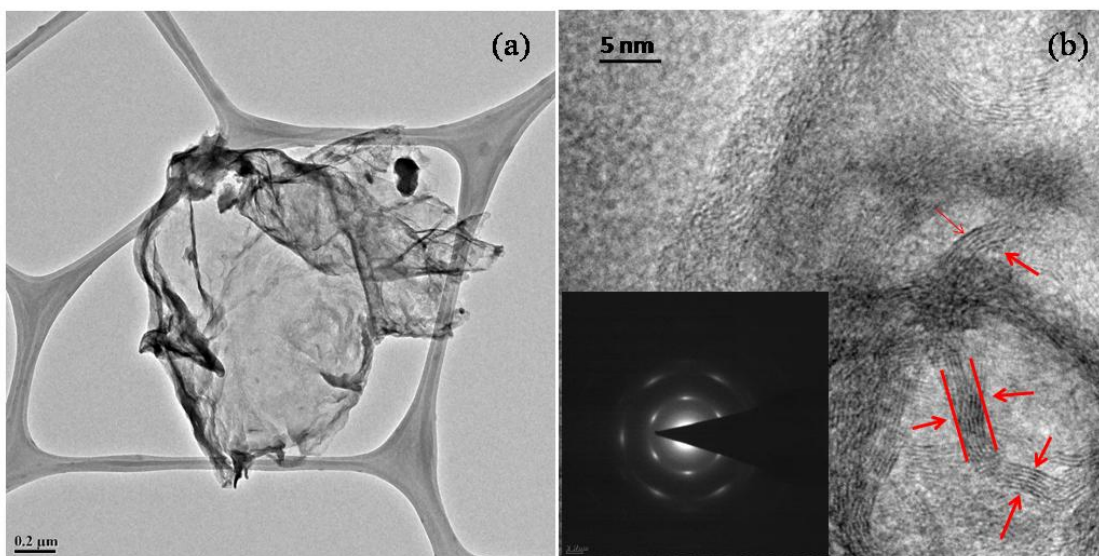


Figure S3. Transmission Electron Microscopic (TEM) images of the PF-1000 electrocatalysts at different magnifications: (a) 0.2  $\mu\text{m}$  and (b) 5 nm scale bar. Inset of (b) shows the selected area electron diffraction pattern of PF-1000.

The HR-TEM images (Figure S3 a) show sheet like structures which confirm that the polymer derived carbon is graphene. Moreover, the obtained lattice fringes of PF-1000 clearly indicate the multilayered nature of the graphene sheets. The selected area electron diffraction pattern of PF-1000 shows a clear hexagonal pattern, which suggests the existence of the different orientations of the crystalline planes due to the crumbling of the multi-layered graphene sheets.<sup>S11</sup>



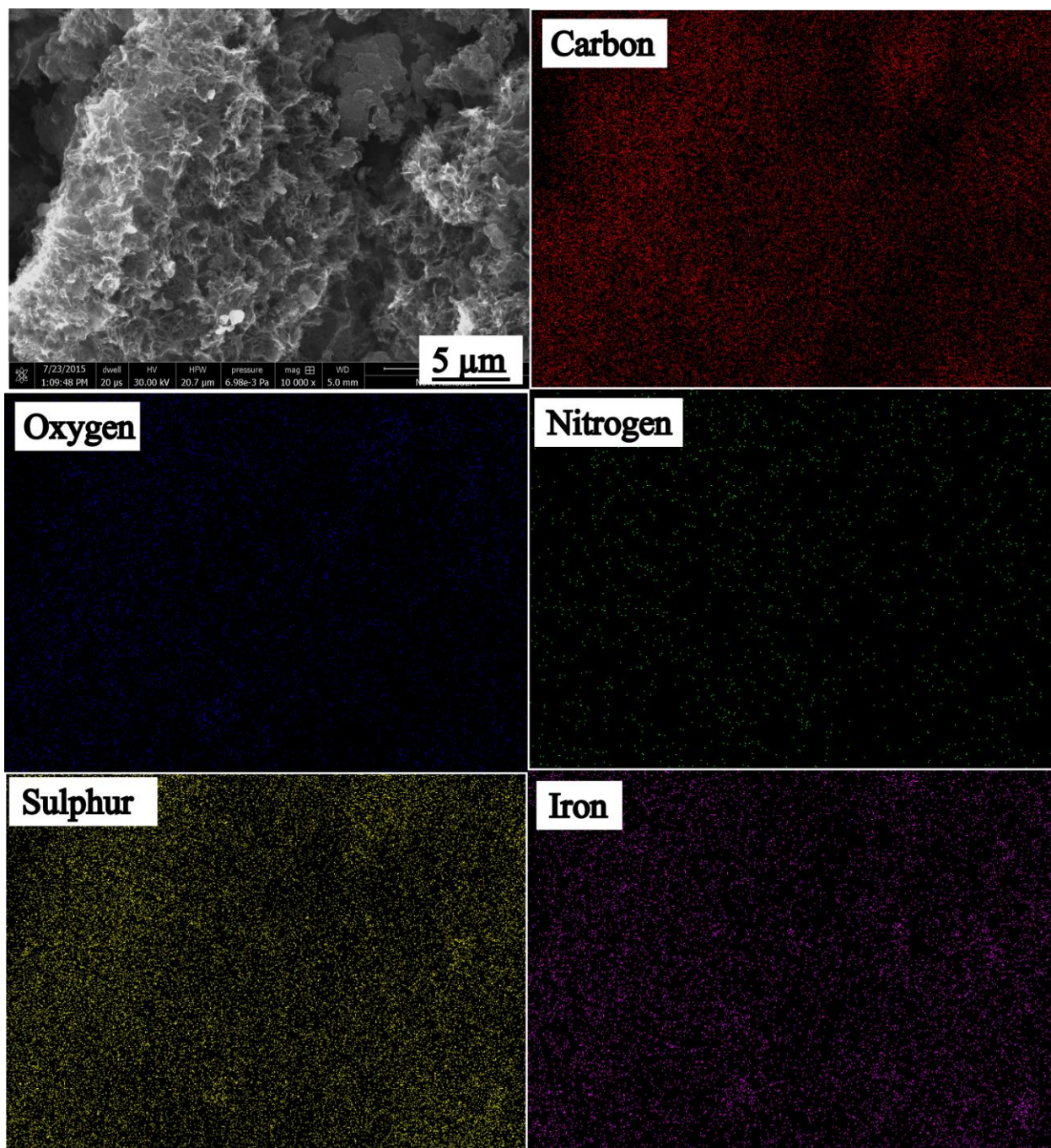


Figure S4. Elemental mapping of PF-1000 using SEM.

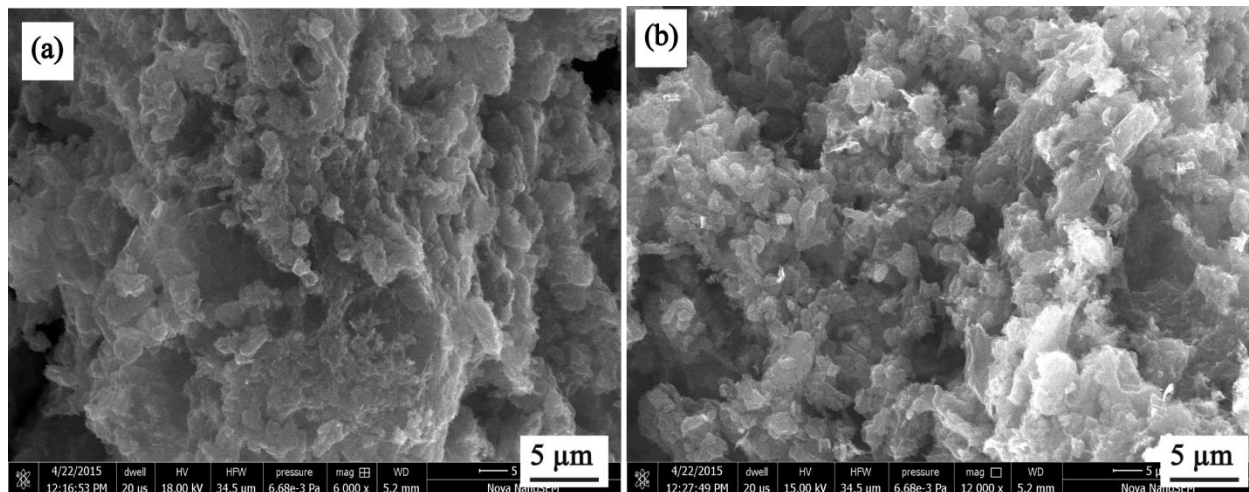


Figure S5. Scanning Electron Microscopic (SEM) images of (a) PF-800 and (b) PF-900.

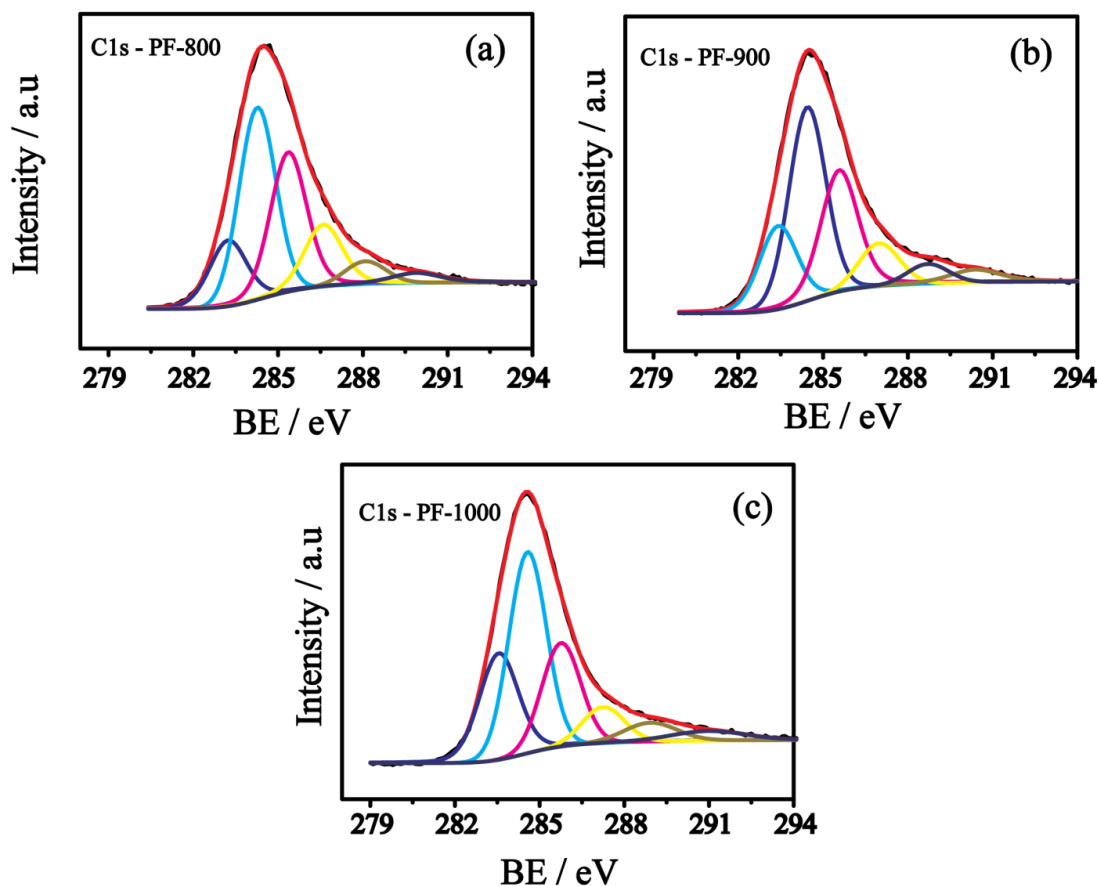


Figure S6. Fitted C1s spectra of (a) PF-800, (b) PF-900, and (c) PF-1000.

The C1s spectrum of PF-1000 was fitted to get an insight on the different types of carbon bondings on the surface. A peak at 283.5 eV observed is corresponding to the metal carbide and the peak at 284.5 eV is attributed to the C=C interaction. Moreover, the indication of the nitrogen and sulphur doping could also be obtained from the peaks at 285.7 eV and 287.3 eV, respectively. The peak at 288.6 eV of the fitted C1s spectra also provides information about the

-O-C=O type interaction of the carbon. The similar peaks are also observed in the PF-800 and PF-900 samples.

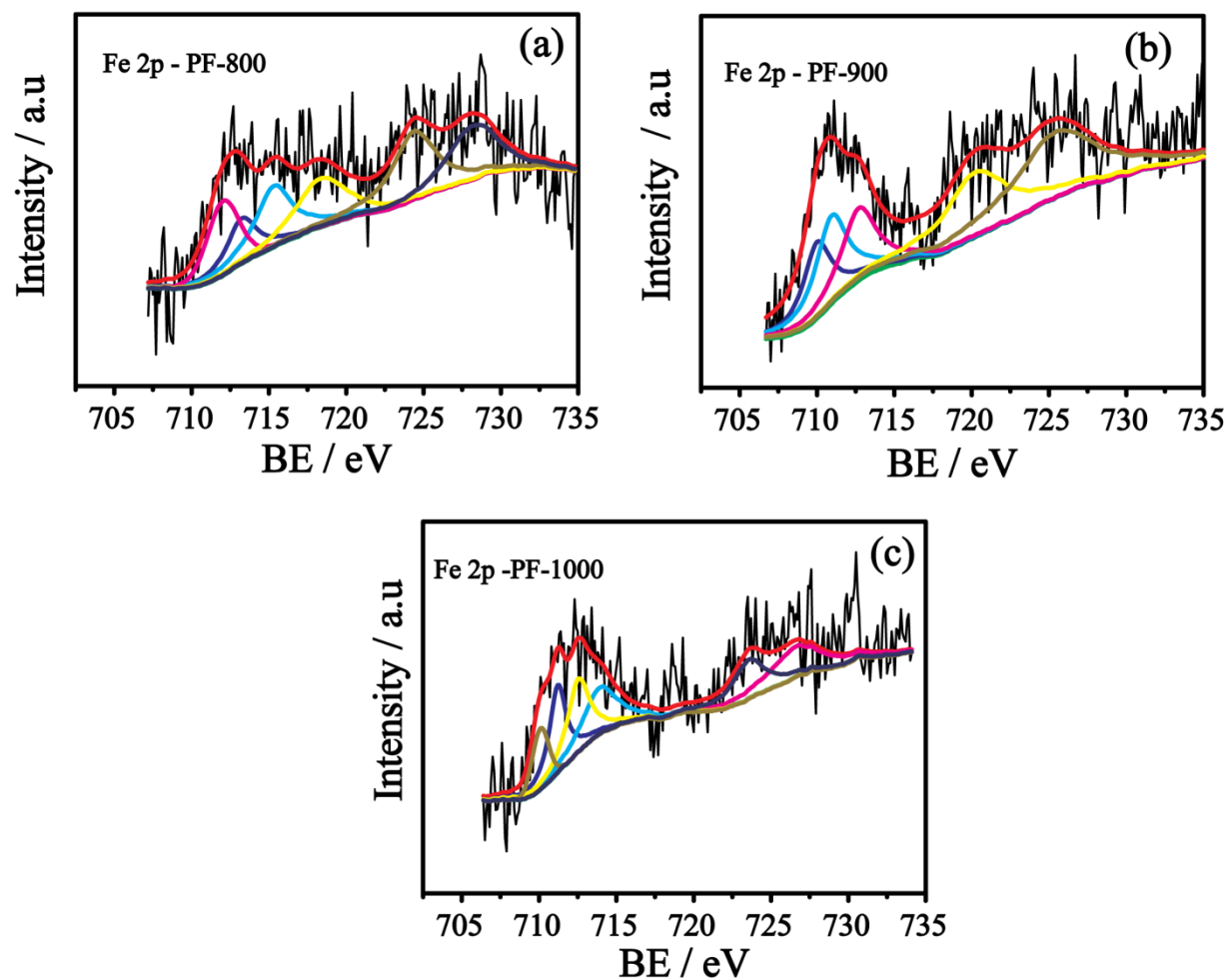


Figure S7. Fitted Fe 2p spectra of (a) PF-800, (b) PF-900, and (c) PF-1000.

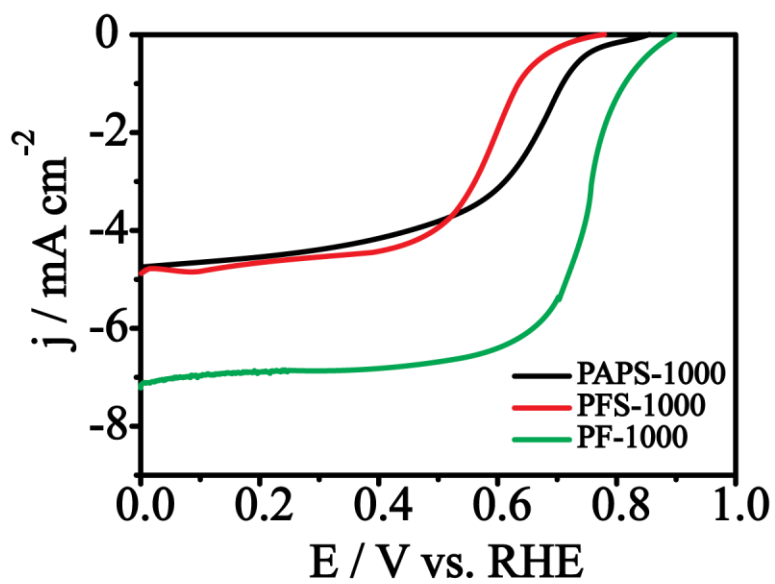


Figure S8. LSVs of PAPS-1000, PFC-1000 and PF-1000 recorded at an electrode rotation rate of 1600 rpm at  $10 \text{ mV s}^{-1}$  scan rate in oxygen saturated  $0.5 \text{ M H}_2\text{SO}_4$ .

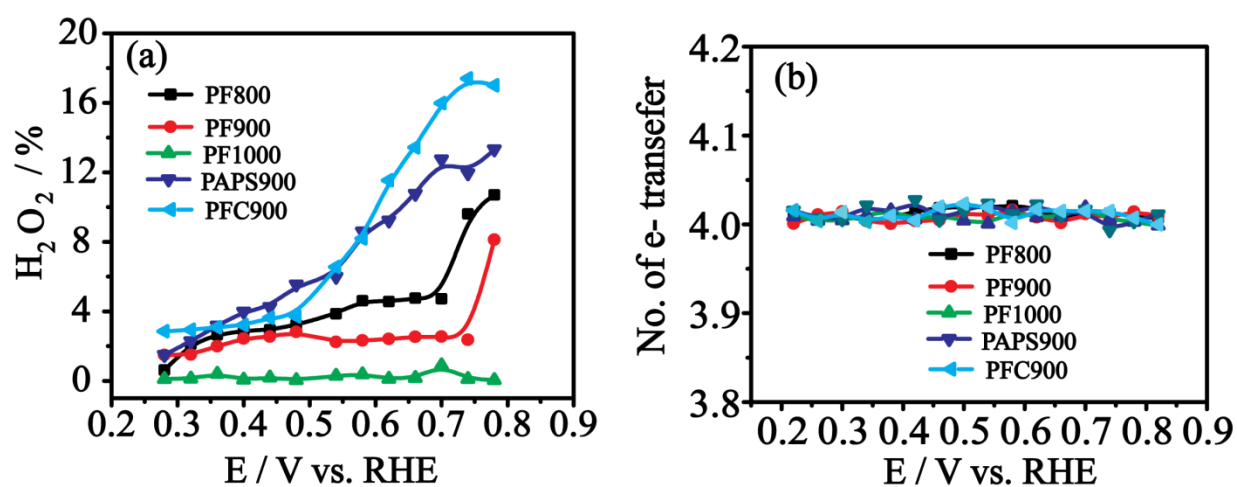


Figure S9. (a) Hydrogen peroxide yield and (b) the number of the electrons transferred in the case of the PF electrocatalysts at different potentials in 0.5 M H<sub>2</sub>SO<sub>4</sub> calculated from RRDE.

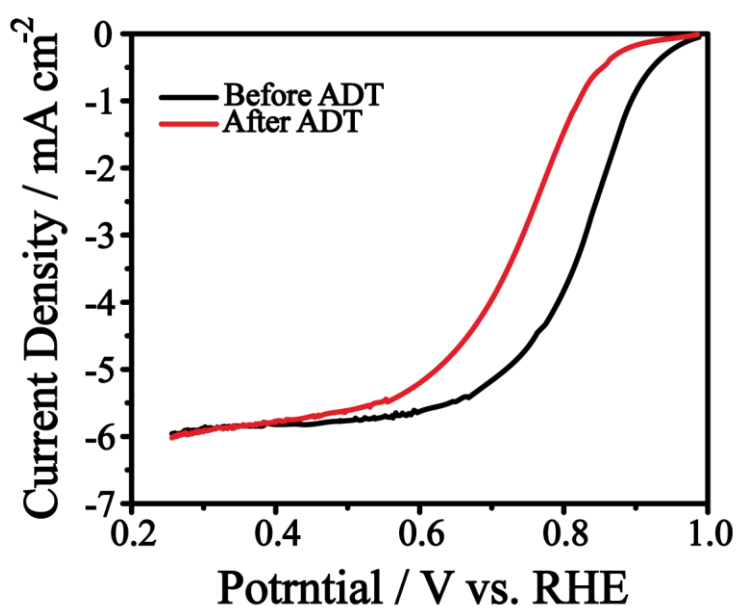


Figure S10. LSVs of Pt/C before and after ADT in 0.5 M HClO<sub>4</sub> at a scan rate of 10 mV s<sup>-1</sup> and an electrode rotation speed of 1600 rpm.

## References

- S1. S. M. Unni, R. Illathvalappil, S. N. Bhang, H. Puthenpediakkal and S. Kurungot, ACS Appl. Mater. Interfaces, 2015, 7, 24256-24264.

- S2. D. Susac, L. Zhu, M. Teo, A. Sode, K. C. Wong, P. C. Wong, R. R. Parsons, D. Bizzotto, K. A. R. Mitchell and S. A. Campbell, *J. Phys. Chem. C*, 2007, 111, 18715-18723.
- S3. B. P. Vinayan, T. Diemant, R. J. Behm and S. Ramaprabhu, *RSC Adv.*, 2015, 5, 66494-66501.
- S4. J. Shi, X. Zhou, P. Xu, J. Qiao, Z. Chen and Y. Liu, *Electrochim. Acta*, 2014, 145, 259-269.
- S5. Y. She, Z. Lu, M. Ni, L. Li and M. K. H. Leung, *ACS Appl. Mater. Interfaces*, 2015, 7, 7214-7221.
- S6. H. Wang, Y. Liang, Y. Li and H. Dai, *Angew. Chem. Int. Ed.*, 2011, 50, 10969-10972.
- S7. M.-Q. Wang, W.-H. Yang, H.-H. Wang, C. Chen, Z.-Y. Zhou and S.-G. Sun, *ACS Catal.*, 2014, 4, 3928-3936
- S8. G. Wu, C. M. Johnston, N. H. Mack, K. Artyushkova, M. Ferrandon, M. Nelson, J. S. Lezama-Pacheco, S. D. Conradson, K. L. More, D. J. Myers and P. Zelenay, *J. Mater. Chem.*, 2011, 21, 11392-11405.
- S9. Q. Li, G. Wu, D. A. Cullen, K. L. More, N. H. Mack, H. T. Chung and P. Zelenay, *ACS Catal.*, 2014, 4, 3193-3200.
- S10. K. P. Singh, E. J. Bae and J.-S. Yu, *J. Am. chem. Soc.*, 2015, 137, 3165-3168.
- S11. H. Huang, Y. Xia, X. Tao, J. Du, J. Fang, Y. Gan and W. Zhang, *J. Mater. Chem.*, 2012, **22**, 10452-10456.